Defence Technology 13 (2017) 119–126

Contents lists available at ScienceDirect

Defence Technology

journal homepage: www.elsevier.com/locate/dt

Ignition and combustion of pyrotechnics at low pressures and at temperature extremes

Clive Woodley*, R. Claridge, N. Johnson, A. Jones

QinetiQ, MOD Fort Halstead, Sevenoaks, Kent, TN14 7BP, United Kingdom

ARTICLE INFO

Article history:
Received 16 December 2016
Received in revised form
17 March 2017
Accepted 27 March 2017
Available online 28 March 2017

Keywords:
Pyrotechnic countermeasure decoy flare
Ignition delay
High altitude chamber
Ignition model
Transport properties

ABSTRACT

Rapid and effective ignition of pyrotechnic countermeasure decoy flares is vitally important to the safety of expensive military platforms such as aircraft. QinetiQ is conducting experimental and theoretical research into pyrotechnic countermeasure decoy flares. A key part of this work is the development and application of improved models to increase the understanding of the ignition processes occurring for these flares. These models have been implemented in a two-dimensional computational model and details are described in this paper. Previous work has conducted experiments and validated the computational model at ambient temperature and pressure. More recently the computational model has been validated at pressures down to that equivalent to 40,000 feet but at ambient temperature (~290 K). This paper describes further experimental work in which the ignition delays of the priming material in inert countermeasure decoy flares were determined for pressures down to 40,000 feet and at temperature extremes of −40 °C and 100 °C. Also included in this paper is a comparison of the measured and predicted ignition delays at low pressures and temperature extremes. The agreement between the predicted and measured ignition delays is acceptable.

1. Introduction

Rapid and effective ignition of pyrotechnic countermeasure decoy flares is vitally important to the safety of expensive military platforms such as aircraft. Ignition needs to be rapid and consistent for the countermeasure to be effective. QinetiQ is conducting experimental and theoretical research into pyrotechnic countermeasure decoy flares. A key part of this work is the development and application of improved ignition models to improve the understanding of the ignition processes occurring for these flares. Typically, pyrotechnic countermeasure decoy flares are wrapped in a material such as foil. Until this material bursts or ruptures, the flare can be considered to be effectively a closed system. Therefore it is possible to use gun internal ballistics models to investigate the ignition and combustion processes in these flares.

Improved ignition models have been implemented in a two-dimensional (2D) gun internal ballistics code named QIMIBS (QinetiQ Modular Internal Ballistics Software) [13]. QIMIBS contains models of the convective, radiative, condensative and conductive heat transfer processes from the igniter combustion products to the main propellant, in this case the flare body. An intensive modelling work programme, closely supported by experiments to provide data for and to validate the modelling, was undertaken for a baseline pyrotechnic flare. The modelling investigated the main heat transfer processes to determine the dominant energy transfer modes and ways by which the ignition delay of the flares could be decreased.

Previous work has reported on the development, verification and validation of the heat transfer models embodied in QIMIBS [11]. This work has been conducted at 21 °C and at atmospheric pressure (0.1 MPa) only.

Further modelling work has been conducted using results from experiments conducted by Esterline in a high altitude chamber (HAC) [12] and by QinetiQ in a modified vacuum oven. The HAC is capable of reducing the ambient pressure to that equivalent to an altitude of 40,000 feet (12,192 m, 0.0188 MPa). Tests of inert pyrotechnic countermeasure decoy flare bodies containing a priming material were conducted in the HAC at pressures equivalent to sea level, 20,000 feet (6096 m, 0.0466 MPa) and 40,000 feet. The tests were recorded using a high speed video camera. The modified vacuum oven is capable of operating at pressures similar to those of the HAC and, in addition, at temperatures in the range -40-100 °C.

* Corresponding author.
E-mail address: cliverwqq@gmail.com (C. Woodley).
Peer review under responsibility of China Ordnance Society.

http://dx.doi.org/10.1016/j.dt.2017.03.004

QIMIBS was used to model these tests and to predict the ignition delay of the priming material. The QIMIBS predictions and measured data were in good agreement.

This paper reviews the models and energy transfer equations important to the requirement to model the ignition of energetic materials. It then describes the experiments and computer modelling carried out. Note that this paper concentrates on the ignition process of the priming material; hence inert flare bodies were used.

2. Ignition model

The ignition of an energetic material is a very complex process, involving many factors. Any ignition model should take into account the following factors:

- Thermal properties of the material to be ignited;
- Transport properties of the igniter gases;
- Convective, radiative, conductive and condensative heating of the material to be ignited;
- Melting of components;
- Latent heat of melting;
- Vaporisation of components;
- Latent heat of vaporisation;
- Subsurface chemical reactions – these can be endothermic or exothermic;
- Gas phase chemical reactions – these can also be endothermic or exothermic;
- Multi-phase flow.

To model all of these processes would require a substantial model development and validation process which is beyond the scope of available resources. Furthermore, although key chemical reaction steps in the ignition of some energetic materials are known, in general such information is not available in the open literature, if known at all. Even if such information was known and implemented in a computational code, the execution of it would take many hours and probably days, even on computer systems having parallel processors. Consequently, assumptions on the ignition process are usually made in order to develop a tractable "engineering" level computational model. It is accepted that such a computational model may not be capable of predicting ignition delays to a high degree of accuracy, but is sufficiently accurate to predict broad trends and to compare one ignition system or energetic material with others. Furthermore, such a computational model should be capable of predicting to an acceptable level of accuracy whether ignition will occur – the go/no-go criterion. This second approach has been used by QinetiQ in the UK to investigate and improve its understanding of the ignition of pyrotechnic countermeasure decoy flares. A very good review of solid propellant ignition models and their suitability for the internal ballistics modelling of guns has been given by Ref. [8].

QinetiQ has developed and used for many years a two-dimensional (2D), inviscid, multi-phase flow internal ballistics code named QIMIBS. QIMIBS uses equations typical of many computational fluid dynamic codes with combustion. It solves equations expressing the conservation of mass, momentum and energy in two dimensions using Riemann solvers. Solid phases are represented as a fluid. A key part of the development of QIMIBS has been to implement ignition submodels describing convective and radiative heating processes. However, it has been shown in experiments that non-gaseous combustion products from the igniter play a significant role in the ignition process [9]. Also, many pyrotechnics use energetic materials in the ignition train that produce mostly non-gaseous combustion products. Therefore, to improve the ignition modelling capabilities of QIMIBS for guns and to allow it to be used to model the ignition of rockets and pyrotechnics, submodels for heating due to conductive and condensative processes were developed and implemented.

QIMIBS models the heat input at the surface of the propellant grain and predicts the flow of heat within the grain using a standard one-dimensional heat conduction model. Ignition at the propellant surface is assumed to occur when the surface temperature exceeds a value specified by the user. This temperature is usually based on that measured in differential scanning calorimetry (DSC) tests, for example.

2.1. Convective heating model

This model is similar to that described and used in the United States Army Research Laboratory NOVA code [7].

The convective heat transferred to the solid propellant is given by Eq. (1)

$$q_c = h_v(T_g - T_s) \tag{1}$$

where q_c is the convective heat flux, h_v is the convective heat transfer coefficient, T_g is the gas temperature and T_s is the surface temperature of the solid propellant. In some codes, the gas temperature is replaced by a temperature known as the film temperature. The film temperature is the arithmetic average of the gas temperature and the propellant surface temperature. Use of a film temperature attempts to account for the possible presence of an insulating boundary layer near the propellant surface. However, no physical justification has been found for using an average of the gas and propellant surface temperatures. The use of the film temperature rather than the gas temperature will be to decrease the heat flux to the solid propellant (identical heat flux at ambient conditions but decreasing logarithmically with temperature to be 24% lower at 2000K). QIMIBS does not use a film temperature.

The heat transfer coefficient is calculated using the Nusselt number, Nu (Eq. (2)). In Eq. (2), k is the thermal conductivity of the gas evaluated at the gas temperature and D is an effective diameter of the solid propellant. The Nusselt number is effectively a dimensionless temperature gradient in the gas.

$$h_v = h_{v\mathrm{mult}} Nuk/D \tag{2}$$

QIMIBS uses a convective heating multiplier, $h_{v\mathrm{mult}}$, in Eq. (2) to account for inaccuracies in the ignition model or uncertainties in the propellant properties (e.g. the thermal conductivity or ignition temperature) in order to obtain good agreement with measured data for a particular propellant and igniter system. The convective heating multiplier should normally be unity unless experimental evidence indicates it should be increased or decreased.

The Nusselt number is calculated using the correlation of Gelperin and Einstein [5], Eq. (3a), for granular propellant, or Eq. (3b) for stick propellant [2]. The coefficients are likely to vary with surface roughness.

$$Nu = 0.4Re^{2/3}Pr^{1/3} \tag{3a}$$

$$Nu = 0.026Re^{0.8}Pr^{1/3} \tag{3b}$$

where *Re* is the Reynolds number and *Pr* is the Prandtl number. Eq. (3a) assumes the propellant bed is fluidised. When a fluid passes through a packed bed, it has been found that at a critical velocity (dependent on many factors such as fluid properties, particle geometry, etc) the fluid begins to carry the particles so that they start moving apart – at this point the bed is in a fluidised state. For non-

fluidised beds (packed beds), the Denton correlation [3] is used – the only difference is that the Reynolds number is raised to the power of 0.7 in Eq. (3a). In QIMIBS it is assumed that the propellant bed quickly becomes in a fluidised state.

The gas thermal conductivity is calculated, using the definition of the Prandtl number, from Eq. (4), where c_p is the gas specific heat at constant pressure and μ is the gas dynamic viscosity evaluated at the gas temperature.

$$k = c_p \mu / Pr \tag{4}$$

The gas dynamic viscosity is calculated using Sutherland's formula [10], which is shown in Eq. (5). The constants in Eq. (5) are applicable for air – in QIMIBS the user can replace them by constants (if known) more appropriate for the igniter used.

$$\mu = (1.458E-6)\frac{T_g^{3/2}}{T_g + 110.33} \tag{5}$$

The Reynolds number, *Re*, is a non-dimensional number that represents the ratio of pressure forces to viscous forces in a flow. It is calculated using (6)

$$Re = \rho_g |u_g - u_s| D/\mu \tag{6}$$

where ρ_g is the gas density, u_g is the gas velocity and u_s is the solid propellant velocity.

The Prandtl number characterises the mode of thermal convection and is dimensionless. It is calculated from Eq. (7) where γ is the ratio of specific heats for the gas [4]. Using Eq. (7), the Prandtl number is independent of temperature and pressure, assuming fixed thermodynamic parameters.

$$Pr = \frac{\gamma}{2.25\gamma - 1.25} \tag{7}$$

The gas specific heat capacity at constant pressure is calculated from Eq. (8) where R is the Universal gas constant and M_w is the mean molecular weight of the products of combustion.

$$c_p = \frac{\gamma . R}{(\gamma - 1) M_w} \tag{8}$$

The original work that determined the Nusselt number correlations used packed beds of spheres. It was found that the same relationships could be used for beds composed of more irregularly shaped particles as long as their shape did not deviate too much from that of a sphere. Instead of using the particle diameter as the effective diameter in Eq. (2), the effective diameter is calculated from Eq. (9), where V and A are the volume and surface area respectively of a single grain.

$$D = 6V/A \tag{9}$$

In some other codes, alternative equations to those stated for Eq. (3a) and Eq. (3b) are used. In some cases, the same Nusselt number correlations are used for both granular and stick propellant beds. An alternative to Eq. (3a) for a packed bed uses a coefficient of 0.8 instead of 0.4. An alternative to Eq. (3b) uses a coefficient of 0.023 instead of 0.026 and a Prandtl number exponent of 0.4 instead of one third.

Modellers of rocket internal ballistics use a slightly different approach to that described above for QIMIBS. Rather than calculate the gas thermal conductivity from Eq. (4) and the gas dynamic viscosity from Eq. (5), a thermochemical equilibrium code is used to calculate both quantities and then the Prandtl number is calculated using Eq. (4).

2.2. Radiative heating model

The convective heat transferred to the solid propellant is given by Eq. (10)

$$q_r = \varepsilon\sigma\left(T_g^4 - T_s^4\right) \tag{10}$$

where q_r is the radiative heat flux, ε is the energetic material emissivity, σ is the Stefan–Boltzmann constant, T_g is the gas temperature and T_s is the surface temperature of the solid propellant.

2.3. Conductive and condensative heating model

Details on this have been given elsewhere and will only be summarized in this paper [13]. A particle–particle interaction model has been developed, implemented into QIMIBS, tested and takes into account the following factors:

- Porosities of solid propellant and non-gaseous products of combustion;
- Interphase slip velocity;
- Probability of collisions;
- Energy released following a collision.

Fig. 1 illustrates the model used and the main features of it are:

- An igniter product species and a solid propellant species are defined;
- Species have different velocities and sizes and can collide (the example shows both species are spherical and have the same diameter);
- The collision rate per unit volume = $n_1 n_2 \pi d^2 |v_2 - v_1|$;
- The igniter product species sticks (and stays stuck) to the solid propellant species, liberating energy.

The model implemented uses a probability factor to allow for the possibility that some collisions do not result in the igniter product species sticking to the solid propellant. This probability factor is a user-defined parameter and would be unity if all collisions resulted in 'sticking'. The probability of an igniter product sticking to a solid propellant grain will depend on the nature of the igniter product (e.g. whether it is liquid or solid), the velocity difference and the softness of the solid propellant grain. A solid igniter product is more likely to imbed itself in a soft propellant grain, and bounce off a hard propellant grain.

A second key input parameter required for the interaction model is the energy released on impact. This is dependent on the energy in the non-gaseous components of the igniter combustion

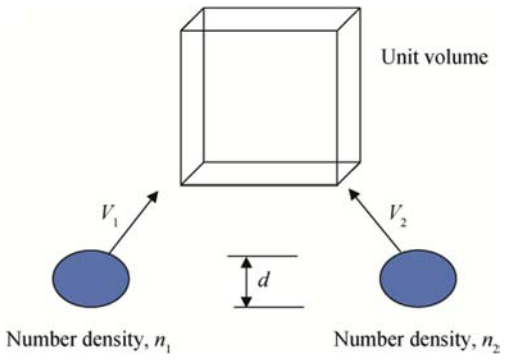

Fig. 1. Particle–particle interaction model.

products. An energy budget analysis needs to be conducted for any igniter. This analysis identifies what products are produced, and how the energy in these products varies with temperature and pressure.

An example of the energy budget analysis calculated for black powder is shown in Fig. 2 and Fig. 3. Fig. 2 shows the predicted variation with temperature of the mass composition of the combustion products of black powder for a pressure of 5 MPa. These were predicted using the Real code [1]. Of key significance is the presence of phase changes such as those for potassium carbonate or potassium sulphide at about 1200 K. At this temperature, as shown in Fig. 3, there is a significant change in the specific energy for potassium sulphide, but not for potassium carbonate. When potassium sulphide components from the black powder combustion products cool then there will be a release of latent energy due to a phase change at 1200 K. If this happens when that species is in contact with energetic material then it will result in a significant heat pulse to that material.

2.4. Effect of igniter gas transport properties

A key part of the ignition model is the effect of the gas transport properties (Prandtl number, viscosity, thermal conductivity and specific heat capacity at constant pressure) on the calculated convective heat transfer coefficient. The transport properties are very dependent on the igniter gas produced and also on the local gas temperature and pressure. Combining equations (2) and (3a) and (6) then it can be seen that

$$h_v \propto \mu^{-2/3} Pr^{1/3} k \tag{11}$$

The Prandtl number characterises the mode of thermal convection and is dimensionless. From Eq. (7), the Prandtl number is independent of temperature and pressure, assuming fixed thermodynamic parameters.

Instead of assuming constant transport properties, QIMIBS allows for the input of a table where they are dependent on both pressure and temperature.

Transport properties can be calculated using thermochemical equilibrium codes such as the NASA (National Aeronautics and Space Administration) Lewis (now Glenn) Research Center CEA2 (Chemical Equilibrium with Applications) code [6] and that is the approach adopted for QIMIBS. The Real code is also used [1]. Investigations conducted by QinetiQ showed that the difference between the convective heat transfer coefficients calculated using the QIMIBS equations together with the transport data predicted by the CEA2 code can be as great as 30%–40%, as indicated in Fig. 4. This shows the variation in the scaled heat transfer coefficient with temperature for black powder at a pressure of 1 bar. The two cases compared are those assuming constant transport property data (Constant values) or allowing the transport data to vary according to temperature and pressure (Varying values).

2.5. Thermal properties of solid propellant

The thermal properties of different energetic materials vary considerably and there is a significant temperature effect, as shown in Fig. 5. Apart from SR57a, all the energetic materials are solid propellants used in guns. SR57a is mainly a mixture of boron and bismuth trioxide.

Thermal conductivity and specific heat capacity measurements were carried out on propellant samples using a modified Du Pont DSC 910 apparatus specially adapted to perform these types of measurement. Unfortunately this equipment is not easily able to be modified to measure the thermal properties at different temperatures. Consequently, although QIMIBS can vary the thermal properties as a function of temperature, constant values for the priming material were used in the modelling. The thermal conductivity and

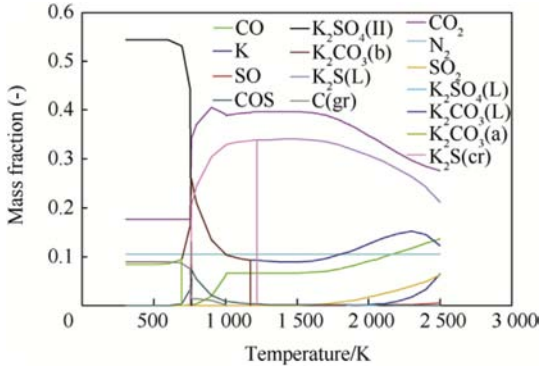

Fig. 2. Mass fraction distribution of combustion products from black powder at 5 MPa.

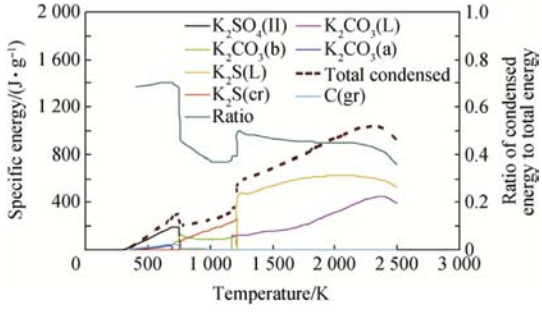

Fig. 3. Specific energy distribution for combustion products from black powder at 5 MPa.

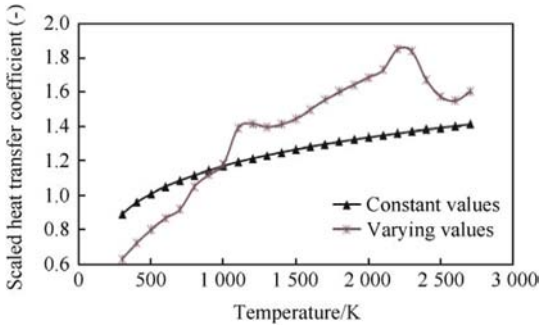

Fig. 4. Scaled heat transfer coefficient assuming constant and varying properties.

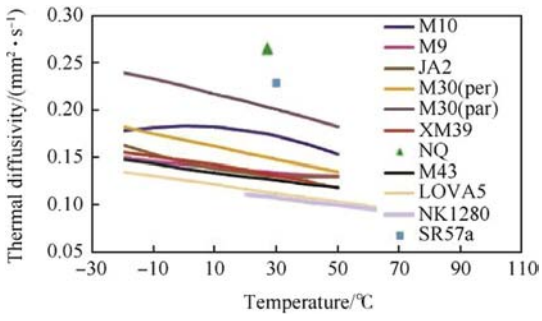

Fig. 5. Thermal diffusivities of different energetic materials.

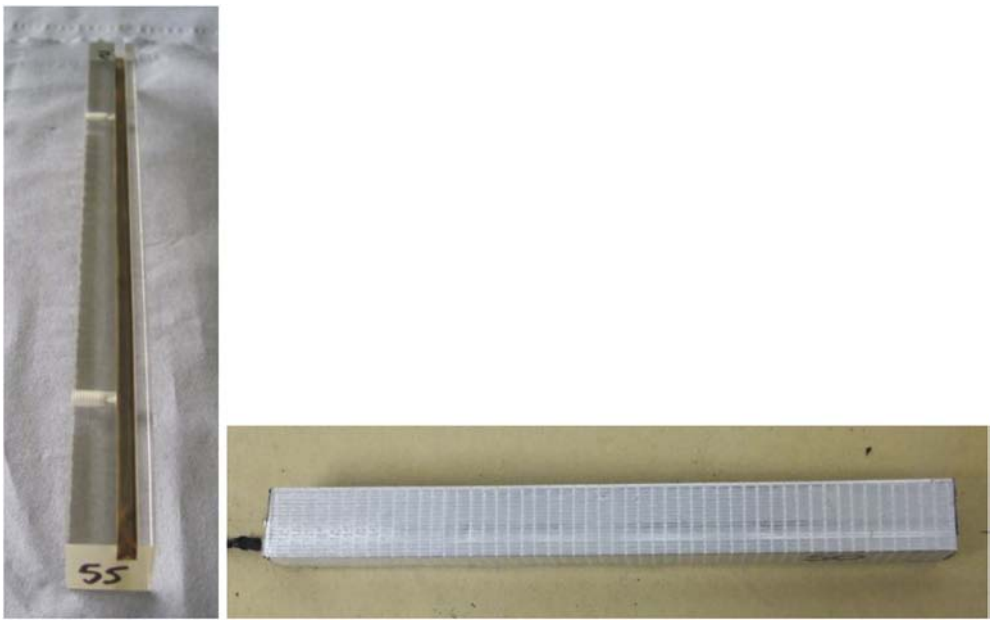

Fig. 6. Inert body primed with WIC 241 (left) and wrapped (right).

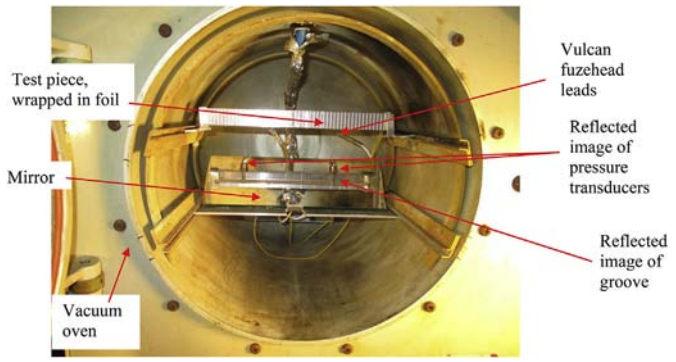

Fig. 7. Trials set-up for hot/cold firings at altitude.

thermal diffusivity measured and used in the modelling were 1.245 W/m/K and 0.856 mm^2/s, respectively.

3. Ignition test setup and results

Forty countermeasure bodies were tested by QinetiQ to determine the effects of both pressure and temperature (high and low) on the ignition of priming material in grooved Perspex bodies. The inert bodies were manufactured from Perspex® and were representative of a 118 flare geometry (Fig. 6). They were primed with approximately 2 g of WIC (Wallop Industry Composition) 241 (a mixture of magnesium and barium peroxide) in a groove (4.5 mm wide by 6 mm deep by 208 mm long) that ran lengthwise along the body. A pressure tapping was located 40 mm from each end of the pellet. Pressures were measured using a Kulite Semiconductors Model XTEL-190 pressure transducer (maximum rated pressure of 100 psi). Foil wraps supplied by Esterline were used to ensure consistency with in-service devices. The test pieces were wrapped so that the primed groove was completely enclosed and sealed, but the pressure tappings were left clear to allow the free insertion of the pressure gauge. A small amount of QuickMatch (cotton impregnated with black powder), with the paper tubing removed, was placed into the mouth of the priming groove and a Vulcan fusehead was placed on top and sealed into place.

The firings were performed in a modified vacuum oven fitted with a glass door to allow high speed imagery to be performed on the test piece; a mirror was placed beneath the test piece to allow

Table 1
Observed ignition delays from all tests.

Altitude/ft	Temperature/(°C)	Ignition delay/ms
0	−40	146
		105
		105
		95
		124
	14	78
		121
		93
		59
	100	94
		63
		4
		10
20,000	−40	11
		325
		515
		571
		278
	14	304
		109
	100	19
		93
		69
		100
		140
40,000	−40	431
		319
		460
		124
	14	1046
		208
	100	638
		979
		86
		562
		233

Table 2
Mean ignition delays.

Altitude/ft	Temperature/(°C)	Ignition delay/ms
0	−40	115
	14	60
	100	36
20,000	−40	422
	14	206
	100	84
40,000	−40	334
	14	627
	100	500

for two planes to be observed (Fig. 7). The test pieces were conditioned for 3 h prior to functioning. The pressure was reduced in the oven using an external vacuum pump and the pressure was measured using a needle gauge. When the desired pressure was obtained, the vacuum was isolated and the item was functioned. The results from the trials are listed in Table 1 and summarised in Table 2. The measured ignition delays (defined as the time from the firing pulse to the time when a clear flame can be seen in the video) were very variable. This is attributed to variations in the priming process. This was done by hand in order to replicate the normal process used for service munitions. Variations in the priming process will lead to uneven thicknesses which in turn can lead to cracks during the drying process.

Images captured from the high speed imagery of a typical firing are shown in Fig. 8 where (a) shows white sparks from the output of the Vulcan fuse head, (b) output from the Quickmatch and initial ignition of the priming composition (bright white spot indicated on the reflected image), (c) primer composition beginning to travel along the groove, (d) primer composition burning steadily.

Analysis of the data indicates various trends:

- Increasing the temperature at constant altitude reduces the ignition delay;
- Increasing the altitude at constant temperature increases the ignition delay.

However, it is likely that pressure has a larger effect than temperature on the ignition delay; this would be expected as the gas generated could diffuse and escape from the system quicker resulting in less thermal impact.

Only a few firings were performed at ambient temperatures on the QinetiQ trial as these replicated the data from an earlier trial [12].

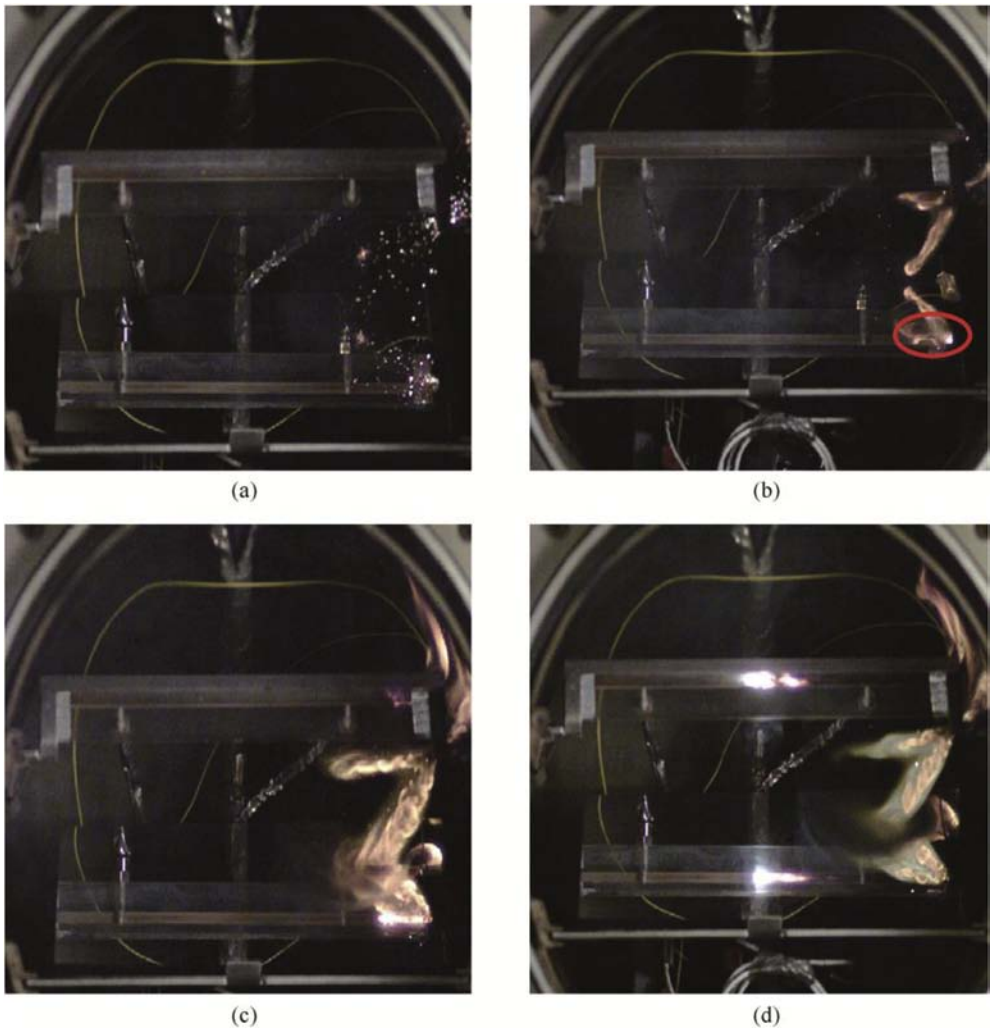

Fig. 8. Frames capture from high speed imagery of priming composition WIC241burning in a wrapped inert flare (a) ignition of Vulcan fusehead, (b) combustion of Quickmatch and takeover of primer, (c) ignition of primer composition in groove, (d) steady burn in groove.

4. Ignition modelling

The main condensed phase combustion products from the Vulcan fusehead and Quickmatch ignition system were predicted to be potassium chloride (KCl), potassium sulphide (K_2S), carbon, potassium carbonate and lead. Typically about 30–40% by mass of the combustion products were condensed.

QIMIBS was used to predict the ignition delays for the firings. Figs. 9 to 14 compare the measured and predicted ignition delays at different altitudes and initial temperatures.

In general the agreement is acceptable. The correct trends are predicted, i.e. the ignition delay increases as the altitude increases and decreases as the initial temperature increases. Unfortunately there is considerable variability in the experimental ignition delays and this has impacted the ability to validate the QIMIBS predictions more completely.

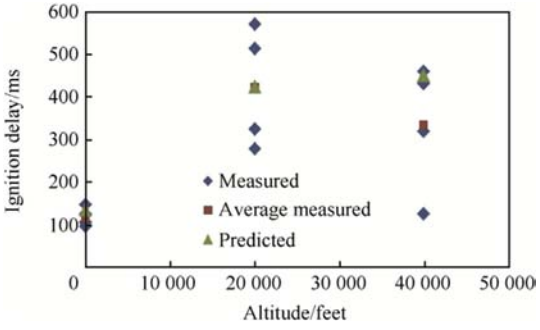

Fig. 9. Measured and predicted ignition delays at −40 °C.

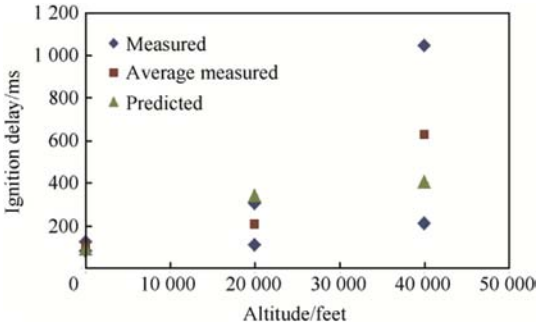

Fig. 10. Measured and predicted ignition delays at 0 °C.

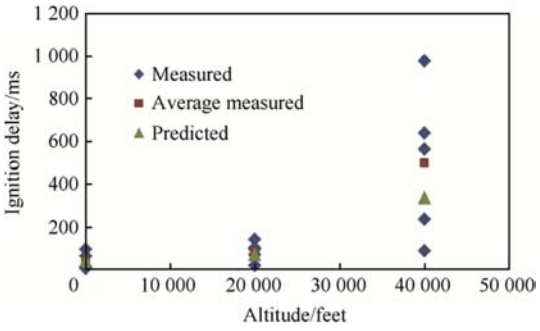

Fig. 11. Measured and predicted ignition delays at 100 °C.

5. Conclusions

Use of a modified vacuum oven fitted with a glass door to allow high speed imagery has enabled investigations into the ignition and burning of primed inert bodies representative of pyrotechnic countermeasure decoy flares. With this equipment, tests can be conducted at temperatures in the range -40-100 °C and pressures as low as that equivalent to an altitude of 40,000 feet.

Measured ignition delays have been compared with those predicted for WIC241 priming composition. In general the agreement is acceptable. The correct trends are predicted, i.e. the ignition delay increases as the altitude increases and decreases as the initial temperature increases.

Further work needs to be conducted to reduce the variability in the experimental ignition delays which has impacted the ability to validate the QIMIBS predictions more completely.

After the experimental variation has been reduced, similar work should be conducted for other materials to validate the ignition modelling further.

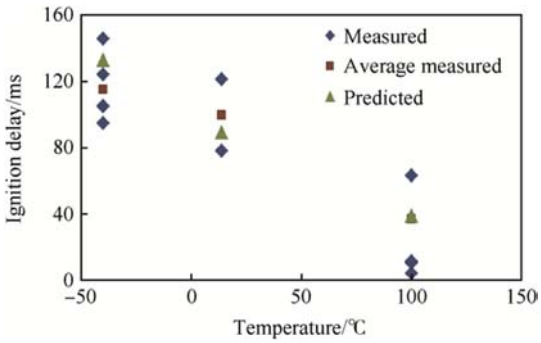

Fig. 12. Measured and predicted ignition delays at 0 feet.

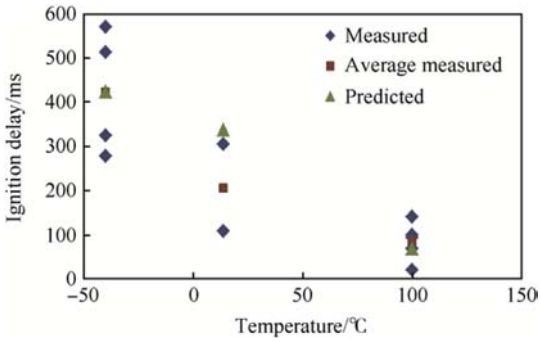

Fig. 13. Measured and predicted ignition delays at 20,000 feet.

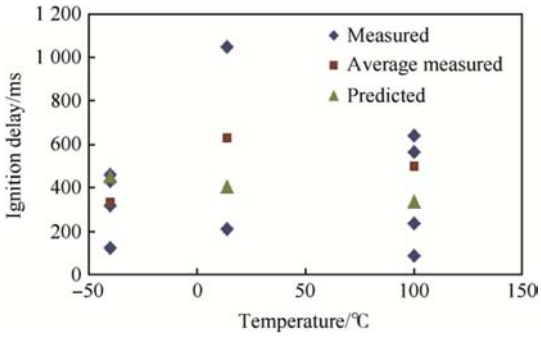

Fig. 14. Measured and predicted ignition delays at 40,000 feet.

Acknowledgement

This research programme was funded by the Defence Science and Technology Laboratory (Dstl), part of the UK MOD, under the Weapons Science and Technology Centre (WSTC).

References

[1] Belov GV. REAL – thermodynamic examination of combustion products under high pressure. In: Proceedings of the 28th ICT conference; 1997 [Karlsruhe, Germany].
[2] Bird RB, Stewart WE, Lightfoot EN. Transport phenomena, pages 396-407. John Wiley & Sons; 1960.
[3] Eckert ERG, Drake EM. Analysis of heat and mass transfer, pages 413-416. New York: McGraw-Hill; 1972.
[4] Eucken A. Phys Z 1913;14:324.
[5] Gelperin NI, Einstein VG. In: Davidson JF, Harrison D, editors. Heat transfer in fluidized beds, in 'Fluidization'. New York: Academic Press; 1971.
[6] Gordon S, McBride BJ. Computer program for calculation of complex chemical equilibrium compositions and applications I. Analysis, vol. 1311. NASA Reference Publication; 1994. October 1994.
[7] Gough PS. The XNOVAKTC code. BRL-CR-627. February 1990.
[8] Harrland A, Johnston IA. Review of solid propellant ignition models relative to the interior ballistic modelling of gun systems. DSTO-TR-2735. 2012.
[9] Hund M, Volk F, Lenji ML. Influence of the reaction products of ignition powders of the ignition behavior of a surface coated gun propellant. In: Proceedings of the 4th international symposium on ballistics; 1978 [Monterey].
[10] Toro EF. Riemann solvers and numerical methods for fluid dynamics. Springer-Verlag; 1997.
[11] Woodley C, Claridge R, Williams M. Modelling the ignition of pyrotechnic countermeasure decoy flares. In: Proceedings of the 27th international symposium on ballistics; 2013. Freiburg, Germany, April 2013.
[12] Woodley C, Claridge R, Gibbons L, Batchem A, Hughes R. Ambient gas pressure effects on the ignition of pyrotechnic countermeasure decoy flares. In: Proceedings of the 29th international symposium on ballistics; 2016. Edinburgh, UK, May 2016.
[13] Woodley C. Modelling the effects of non-gaseous igniter combustion products on the ignition of gun propellants. In: Proceedings of the 26th international symposium on ballistics; 2011. Miami, September 2011.